SHEAR WAVE VELOCITY-BASED LIQUEFACTION RESISTANCE EVALUATION: SEMI-THEORETICAL CONSIDERATIONS AND EXPERIMENTAL VALIDATIONS

Yun-Min Chen[1], Yan-Guo Zhou[2] and Han Ke[3]

[1] *Professor, MOE Key Laboratory of Soft Soils and Geoenvironmental Engineering, Zhejiang University, Hangzhou 310027, P. R. China*
[2] *Assistant Professor, MOE Key Laboratory of Soft Soils and Geoenvironmental Engineering, Zhejiang University, Hangzhou 310027, P. R. China*
[3] *Associate Professor, MOE Key Laboratory of Soft Soils and Geoenvironmental Engineering, Zhejiang University, Hangzhou 310027, P. R. China*
Email: chenyunmin@zju.edu.cn, qzking@zju.edu.cn

ABSTRACT :

Shear wave velocity measurements provide a promising approach to liquefaction resistance evaluation of sandy soils. Although various relationships between shear wave velocity (V_s) and liquefaction resistance (*CRR*) have been developed, most of them are phenomenological rather than physically-based. In this study, semi-theoretical considerations are given and predict a soil-type specific relationship between *CRR* and V_s normalized with respect to the minimum void ratio, confining stress and exponent n of Hardin equation. Undrained cyclic triaxial test and dynamic centrifuge model test were performed on sands with V_s measured by bender elements to verify this relationship. Further investigation on similar laboratory studies resulted in a large database of sandy soils, which reveals that *CRR* is proportional to the 4 power of V_s at statistical level. Comparisons with field case histories show that the present lower-bound *CRR*-V_s curve is a reliable prediction of liquefaction resistance for most sandy soils, while the accurate evaluation for a specific site requires the development of site-specific liquefaction resistance curve.

KEYWORDS: Liquefaction, Shear wave velocity, Dynamic centrifuge test, Bender elements, Soil-type specific, Relationship

1. INTRODUCTION

Predicting the liquefaction resistance (*CRR*) of soils is an important aspect of geotechnical earthquake engineering. Shear wave velocity (V_s) offers engineers a promising alternative tool to evaluate liquefaction resistance of soils with lower cost and more physically meaningful measurements. The use of V_s as an index of liquefaction resistance is soundly based because both V_s and *CRR* are similarly but not proportionally influenced by many of the same factors, and the advantages of V_s-based method have been comprehensively discussed by many researchers (Youd et al. 2001).

Nowadays the most prevailing approach is in-situ V_s measurements at sites shaken by earthquakes (Andrus and Stokoe 2000), which follows the traditional framework of the Seed-Idriss simplified procedure (Seed and Idriss 1971), and correlates the overburden stress-corrected shear wave velocity (V_{s1}) to the magnitude-scaled uniform cyclic stress ratio (*CSR*) induced by earthquakes. However, the applicability of in-situ method is still limited mainly due to the lack of field performance data (Boulanger et al. 1997). Besides, such methods usually do not produce samples for soil identification, and most of the measured soil parameters accompanying in-situ V_s measurement are post-earthquake properties. Thus despite their practical importance, the field empirical CRR-V_{s1} correlations do not furnish insight into the fundamentals of liquefaction phenomenon. Fortunately, the controlled laboratory liquefaction tests reflect the essence of liquefaction, and could be used to broaden the applicability of liquefaction criteria (Hatanaka et al. 1997). Similar to in-situ methods, the V_s-based laboratory approach for assessing liquefaction resistance involves development of a relationship between shear wave velocity and the liquefaction resistance (CRR_{tx}). Various CRR-V_s relationships were proposed based on liquefaction tests (De Alba et al. 1984; Wang 2001; Wang and Cheng 2005). However, these quantitative findings are essentially phenomenological rather than physically-based, so that these CRR-V_s relationships take different forms and difficult to choose for practical use.

The main purpose of this study is to establish a physically-based relationship between shear wave velocity and liquefaction resistance of sandy soils based on semi-theoretical considerations and experimental studies. The concept of this method lies in the fact that soils of the same type which have the same shear wave velocity under the same stress conditions would also have the same liquefaction resistance (Tokimatsu and Uchida 1990). To meet this objective, bender elements were developed based on cyclic triaxial apparatus and centrifuge apparatus (Zhou et al. 2005; Zhou and Chen 2005; Chen and Zhou 2006), where liquefaction tests were performed on sands after V_s measurements. Then a well-defined CRR-V_s correlation is established. Detailed comparisons with field V_s-based criteria validate the reliability of the present CRR-V_s relationship.

2. SEMI-THEORETICAL CONSIDERATIONS

Most previous studies (Finn et al. 1971; Mulilis et al. 1977) indicated that for a given sandy soil, with other conditions unchanged, the undrained cyclic strength will approximately keep constant despite the variation of confining pressure, namely, CRR_{tx} = C, which leads to the following relationship:

$$(\tau_d = \frac{\sigma_d}{2}) \propto \sigma'_m \tag{2.1}$$

where τ_d = cyclic shear stress; σ'_d = cyclic deviator stress; and σ'_m = mean effective confining pressure.

On the other hand, it is generally recognized that the small-strain shear modulus, G_{max}, can be empirically expressed as a function of the mean effective confining stress and void ratio as following (Hardin and Drnevich 1972):

$$G_{max} = AF(e)(\sigma'_m)^n \tag{2.2}$$

where A = empirical constant; n = empirical exponent; e = void ratio and $F(e)$ is void ratio function, which is given by $F(e) = 1/(0.3+0.7e^2)$. Combining Eqns. 2.1 and 2.2, one may obtain

$$(\tau_d = \frac{\sigma_d}{2})^n \propto G_{max} \tag{2.3}$$

To eliminate the effects of soil types, the term G_{max} in Eqn. 2.3 could be normalized with respect to the minimum void ratio (e_{min}). Then dividing both sides of Eqn. 2.3 by $(\sigma'_m)^n$ leads to:

$$\left(CRR_{tx}\right)^n = k\frac{G_{max}}{F(e_{min})}\frac{1}{\left(\sigma'_m\right)^n} \tag{2.4}$$

where k = an introduced constant for expression clarity.

Eqn. 2.4 reveals the direct relationship between cyclic strength and stiffness of sandy soils, based on two generally known aspects of soil mechanics indicated in Eqns. 2.1 and 2.2 (Chen et al. 2005). For clarity, the terms $(CRR_{tx})^n$ and $G_{max}/[F(e_{min})(\sigma'_m)^n]$ are denoted hereafter as "normalized cyclic resistance ratio" and "normalized shear modulus", respectively. Besides, the small-strain shear modulus could also be related to shear wave velocity by

$$G_{max} = \rho V_s^2 \tag{2.5}$$

where ρ is the mass density of soil. Then Eqn. 2.4 is rewritten as

$$CRR_{tx} = \frac{1}{\sigma'_m}\left[k\frac{\rho V_s^2}{F(e_{min})}\right]^{1/n} \tag{2.6}$$

The above derivations indicate that, if the possible relationship in Eqn. 2.4 could be reliably established in laboratory, the corresponding cyclic resistance ratio (CRR_{tx}) can be readily correlated to V_s according to Eqn. 2.6.

3. VALIDATION BY LABORATORY TESTS

3.1. Cyclic Triaxial Test with Bender Elements

According to the abovementioned considerations, undrained cyclic triaxial tests were performed on reconstituted samples of four sands: Fuzhou sand, Tianjin sand, Toyoura sand and Silica sand no. 8. The physical properties and test conditions are listed in Table 3.1, with grain size distribution curves shown in Figure 1. Bender element testing was conducted and the velocity V_s in the specimen can be calculated from the travel time t and the known tip-to-tip separation L between the bender elements as

$$V_s = L/t \tag{3.1}$$

Then the small-strain shear modulus can be calculated according to Eqn. 2.5.

According to the curves of cyclic stress ratio (CSR_{tx}) versus the number of cycles (N_l) to cause 5% double amplitude strain, CRR_{tx} and G_{max} can be obtained directly by evaluating the curves at 15 cycles. Then the data are normalized according to Eqn. 2.4 and plotted in $\{G_{max}/[F(e_{min})(\sigma'_m)^n], (CRR_{tx})^n\}$ space in Figure 2. As shown in Figure 2, although each group of data exhibits a distinctive linear trend with best-fitting slope [e.g., k value in Eqn. 2.4] varying from one to another, they fall in a narrow band. These results accurately echo the aforementioned semi-theoretical considerations, and illustrated the possibility of establishing Eqn. 2.4 based on laboratory tests.

Table 3.1 Physical properties and test conditions of four sands

Sand type	G_s	D_{10} (mm)	U_c	FC (%)	e_{min}	σ'_m (kPa)	D_r (%)	n
Fuzhou sand	2.65	0.13	3.0	0	0.43	50-400	45,60,75	0.507
Tianjin sand	2.69	0.10	1.7	3.7	0.593	50-400	59.6-73.7	0.503
Toyoura sand	2.635	0.10	1.8	0	0.628	100	38.5-79	0.435
Silica sand no.8	2.645	0.03	2.88	50.6	0.721	100	60.3-84.6	0.521

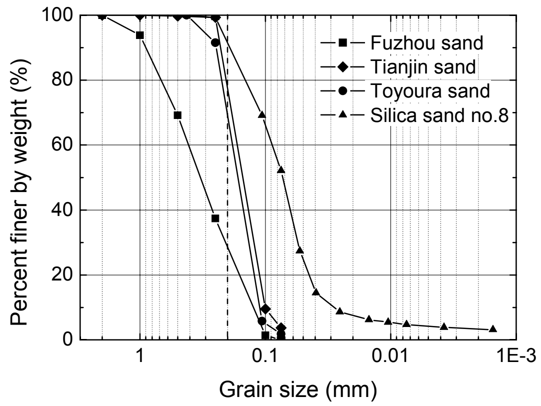

Figure 1 Grain size distribution curves

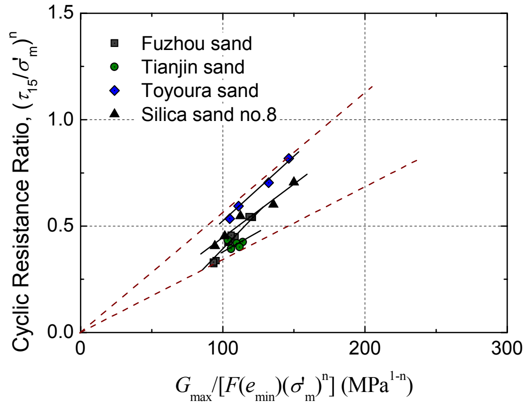

Figure 2 Cyclic triaxial test results

3.2. Database of Laboratory Test

To verify the interesting findings, comprehensive investigation on similar laboratory studies were made. Liquefaction test data of saturated sandy soils, with V_s or G_{max} measured via various laboratory methods (e.g., bender elements, ultrasonic method, high-accuracy sensors etc.), are collected and compiled. This investigation leads to a laboratory database of 296 data points from 35 types of sandy soils, including those of the present tests. According to Andrus and Stokoe (2000), these data can be divided into three classes: 181 are for sands with FC≤5% (class I), 74 for sands with 5%≤FC≤35% (class II) and 41 for silty sands with FC≥35% (class III). All collected data are treated in the same manner as in Figure 2, and plotted in Figure 3.

Similar to but more convincing than Figure 2, data in Figure 3 exhibit linear relationships between $(CRR_{tx})^n$ and $G_{max}/[F(e_{min})(\sigma'_m)^n]$, irrespective of soil types and confining pressures. The final statistics (mean values) for the whole database are: n = 0.506 and e_{min} = 0.60, 0.62 and 0.71 for class I, II, and III, respectively. For a given type of soil, there is only best-fitting k value, while for a database the "lower bound" fitting line is more meaningful. The fitting value (k_{15}) for Silica sand no. 8 and the whole database is 1.50×10^{-4} kPa$^{-0.5}$ and 0.997×10^{-4} kPa$^{-0.5}$ respecitvely.

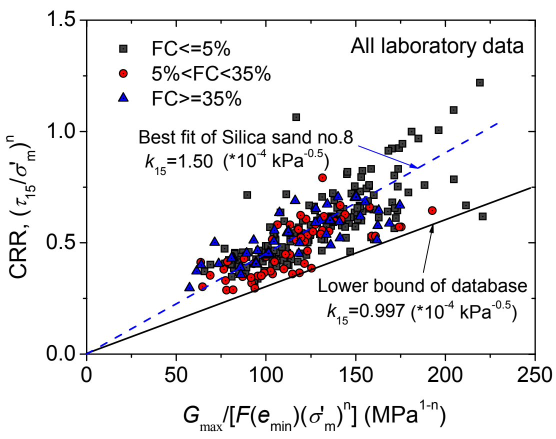

Figure 3 Laboratory database and fitting lines

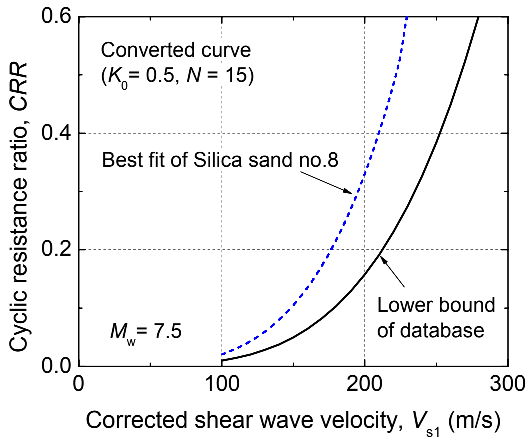

Figure 4 Converted CRR-V_{s1} curves

3.3. Conversion from Laboratory to Field Conditions

It is worth noting that both of the liquefaction resistance (CRR_{tx}) and shear wave velocity (V_s) in Eqn. 2.6 were obtained in undrained cyclic traixial tests under isotropic consolidation conditions, which are essentially different from the in-situ conditions required to be evaluated for design purpose. Therefore it's necessary to convert the laboratory CRR_{tx}-V_s relationship into in-situ applications. According to the common practices (Yoshimi et al. 1989; Robertson et al. 1992), it is readily to convert Eqn. 2.6 into the following form (Zhou and Chen 2007):

$$CRR = r_c \frac{1}{P_a} \left[\frac{k_N \rho}{F(e_{min})} \right]^{1/n} \left(V_{s1} \right)^{2/n} \tag{3.2}$$

Eqn. 3.2 makes it possible to evaluate the liquefaction resistance of in-situ soil deposits with the laboratory test-determined k_N, if the in-situ soil properties such as mass density and minimum void ratio are properly determined.

This semi-theoretical finding has two important implications: the first is, as for a given type of soil, this relationship is strongly soil type-dependent since it requires soil specific parameters such as k_N, exponent n of Hardin equation, minimum void ratio and soil mass density, and this argument has been verified by the aforementioned laboratory tests for four types of sands; the second is, at statistical level, liquefaction resistance of sandy soils will vary proportionally with $(V_{s1})^4$ since n value approximates 0.5 according to the present laboratory database. Based on known parameters such as k_N, n, e_{min} and ρ, the CRR-V_{s1} curves for Silica sand no. 8 and for the lower bound of the whole database in Figure 3 are converted and plotted in Figure 4. It's obvious that these two curves depart from each other. Therefore it's very important to clarify the applicability of the present CRR-V_{s1} curves for liquefaction evaluation under different conditions. The following two sections are to address this issue.

4. VALIDATION BY DYNAMIC CENTRIFUGE MODEL TEST

The main purpose of this section is to verify the accuracy of soil-type specific CRR-V_{s1} relationship for liquefaction assessment based on tests of Silica sand no. 8. Dynamic centrifuge tests were further conducted to simulate seismic liquefaction in level ground and reproduce (CSR, V_{s1}) case histories in model scale, where bender element testing was performed to monitor the soil stiffness before earthquake shaking. By comparing the theoretical CRR-V_{s1} curve of Silica sand no.8 in Figure 4 with the case histories produced by centrifuge tests, the reliability of the present CRR-V_{s1} correlation is verified (Zhou 2007).

The centrifuge model tests were performed using the centrifuge at Institute of Technology, Shimizu Corporation (Sato 1994). Two major testing parameters were varied between experiments: sand relative density D_r (= 61.7-89.8%) and peak input prototype acceleration a_{max} (= 0.05-0.42 g). Bender element system was developed to measure shear wave velocities under high acceleration conditions, and one example of shear wave measurement is illustrated in Figure 5.

All liquefied and non-liquefied data produced by dynamic centrifuge tests are summarized in Figure 6. And the theoretical CRR-V_{s1} curve of Silica sand no. 8 is also plotted in Figure 6. As shown in Figure 6, the theoretical curve separates almost all (about 95%) the liquefied data properly. This model test verified that CRR-V_{s1} curve for liquefaction assessment of a given kind of sand is strongly soil type dependent, which highlights the necessity of developing soil-type specific CRR-V_{s1} correlation for accurate evaluation in critical projects.

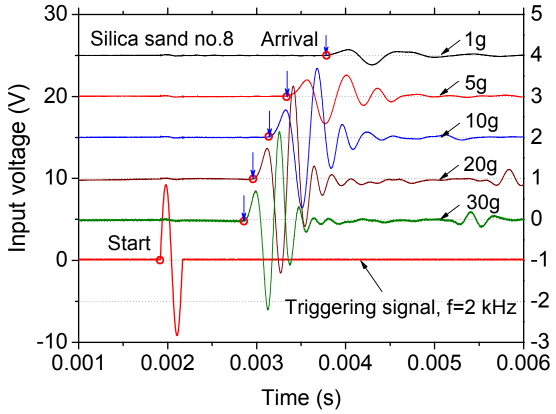

Figure 5 S-wave measurement during swung up

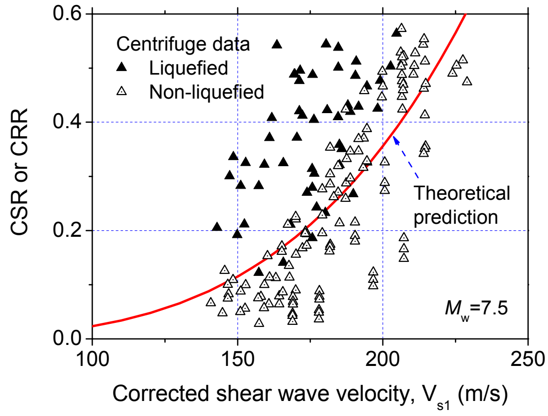

Figure 6 Validation by centrifuge test data

5. COMPARISON WITH FIELD PERFORMANCE DATA

This section will check the reliability of the "lower bound" CRR-V_{s1} curve from laboratory database for preliminary liquefaction evaluation. By assuming n = 0.5, Eqn. 3.2 could be extended accordingly from the soil-type specific perspective to a statistical level with other values determined. That is

$$CRR = r_c \frac{1}{P_a} \left[\frac{k_N \rho}{F(e_{min})} \right]^2 (V_{s1})^4 \tag{5.1}$$

Up until now, the most comprehensive study of in-situ V_s measurements for liquefaction assessment has been presented by Kayen et al. (2004). Figure 7 presents 60% of the global V_{s1} data available, the present lower-bound CRR-V_{s1} curve of FC≤5% and that of Andrus and Stokoe (2000). In view of the in-situ soil conditions, the parameters of Eqn. 5.1 for lower bound curve are adopted as those commonly recommended, that is, r_c = 0.9, e_{min} = 0.65, ρ = 1.90 g/cm^3, k_{15} = 0.997×10^{-4} kPa$^{-0.5}$. The present lower bound curve separates all the liquefied case data properly in a slightly conservative way. Note that in Kayen's database, the Andrus and Stokoe curve of FC≤5% misclassified 6 out of 7 case histories within the zone of CSR>0.3 and V_{s1}>200 m/s. This comparison illustrated the reliability of the present lower bound CRR-V_{s1} relationship for preliminary assessment, especially in the zone of high earthquake intensity and high shear wave velocity. Figure 8 summarizes all CRR-V_{s1} curves of sands with FC≤5% for practical use, in terms of the earthquake magnitude M_w.

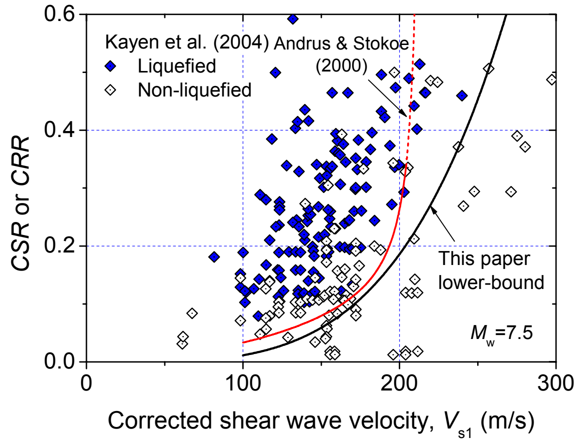

Figure 7 Comparison with global database

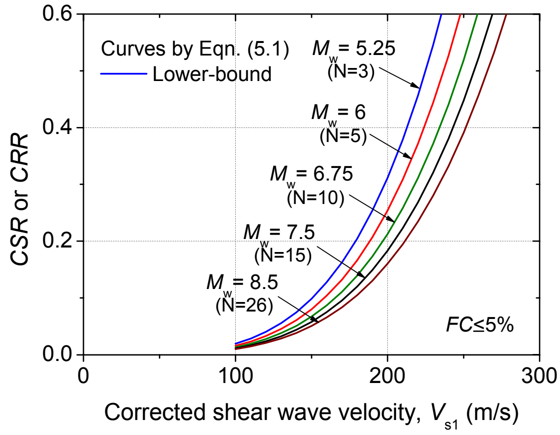

Figure 8 Curves for different magnitudes (FC≤5%)

6. CONCLUSIONS

In this study, semi-theoretical considerations revealed a physically meaningful relationship between liquefaction resistance and shear wave velocity for sandy soils, that is, *CRR* is proportional to the (2/*n*) power of V_{s1}. This finding was then validated by soil element and centrifuge model tests. Comprehensive experiments on Silica sand no. 8 indicated that *CRR*-V_{s1} curve for liquefaction assessment is strongly soil-type dependent. On the other hand, further investigations based on laboratory database of various sandy soils show that, *CRR* will vary proportionally with $(V_{s1})^4$ at statistical level. Comparisons with field case history data show that the present “lower bound” *CRR*-V_{s1} curve agree well with field performance criteria, especially for sites subjected to strong earthquakes (*CSR*>0.3) with high shear wave velocities (V_{s1}>200 m/s). Therefore the present “lower bound” *CRR*-V_{s1} curve from various sandy soils should be treated as a reliable but conservative prediction for most sandy soils and only suitable for preliminary evaluation for a specific site, and the accurate evaluation in engineering practices requires the development of site-specific liquefaction resistance curves from laboratory tests.

ACKNOWLEDGEMENTS

Much of the work described in this paper was supported by the National Basic Research Program of China (No. 2007CB714203) and the Foundation for Seismological Researches, China Earthquake Administration (No. 200808022). The financial supports are greatly appreciated. The authors would also thank Prof. W. D. Liam Finn of University of British Columbia, Prof. Jonathan P. Stewart of University of California (UCLA), and Prof. C. Hsein Juang of Clemson University for their valuable exchanges of ideas and insightful comments about this study.

REFERENCES

Andrus, R.D. and Stokoe, K.H.II. (2000). Liquefaction resistance of soils from shear-wave velocity. *Journal of Geotechnical and Geoenvironmental Engineering*, *ASCE* **126:11**, 1015-1025.

Boulanger, R.W., Mejia, L.H. and Idriss, I.M. (1997). Liquefaction at moss landing during Loma Prieta earthquake. *Journal of Geotechnical and Geoenvironmental Engineering, ASCE* **123:5**, 453-467.

Chen, Y.M. and Zhou Y.G. (2006). Technique standardization of bender elements and international parallel test. *Geotechnical Special Publication No.150*, *ASCE* 90-97.

Chen, Y.M., Ke, H. and Chen, R.P. (2005). Correlation of shear wave velocity with liquefaction resistance based on laboratory tests. *Soil Dynamics and Earthquake Engineering* **25:6**, 461-469.

De Alba, P., Baldwin, K. and Janoo, V., et al. (1984). Elastic-wave velocities and liquefaction potential. *Geotechnical Testing Journal*, *ASTM* **7:2**, 77-87.

Finn, W.D.L., Pickering, D.J. and Bransby, P.L. (1971). Sand liquefaction in triaxial and simple shear tests. *Journal of the Soil Mechanics and Foundations Division*, *ASCE* **97:4**, 639-659.

Hatanaka, M., Uchida, A. and Suzuki, Y. (1997). Correlation between undrained cyclic shear strength and shear wave velocity for gravely soils. *Soils and Foundations* **37:4**, 85-92.

Hardin, B.O. and Drnevich, V.P. (1972). Shear modulus and damping in soils: Design equations and curves. *Journal of the Soil Mechanics and Foundations Division, ASCE* **98:7**, 667-692.

Kayen, R., Seed, R.B. and Moss, R.E., et al. (2004). Global shear wave velocity database for probabilistic assessment of the initiation of seismic-soil liquefaction. *Proc. 11th Int. Conf. On Soil Dynamics and Earthquake Engineering*, 2. Berkeley, CA, 506-512.

Mulilis, J.P., Seed, H.B. and Chan, C.K., et al. (1977). Effects of sample preparation on sand liquefaction. *Journal of the Geotechnical Engineering Division*, *ASCE* **103:2**, 91-108.

Robertson, P.K., Woeller, D.J. and Finn, W.D.L. (1992). Seismic cone penetration test for evaluating

liquefaction potential under cyclic loading. *Canadian Geotechnical Journal*, **29:4**, 686-695.
Sato, M. (1994). A new dynamic geotechnical centrifuge and performance of shaking table tests. *Proc. Int. Conf. Centrifuge 94*, Singapore, 157-162.
Seed, H.B. and Idriss, I.M. (1971). Simplified procedure for evaluating soil liquefaction potential. *Journal of the Soil Mechanics and Foundations Division*, *ASCE* **97:9**, 1249-1273.
Tokimatsu, K. and Uchida, A. (1990). Correlation between liquefaction resistance and shear wave velocity. *Soils and Foundations*, **30:2**, 33-42.
Wang, J.H. and Cheng, G.Y. (2005). Study of correlation between the shear wave velocity and the liquefaction resistance of saturated sands. *Chinese Journal of Geo-technical Engineering* **27:4**, 369-373. (in Chinese)
Wang, W.S. (2001). Utilization of shear wave velocity in assessment of liquefaction potential of saturated sand under level ground during earthquakes. *Chinese Journal of Geotechnical Engineering*, **23:6**, 655-658. (in Chinese)
Yoshimi, Y., Tokimatsu, K. and Hosaka, Y. (1989). Evaluation of liquefaction resistance of clean sands based on high-quality undisturbed samples. *Soils and Foundations*, **29:1**, 93-104.
Youd, T.L., Idriss, I.M. and Andrus, R.D., et al. (2001). Liquefaction resistance of soils: summary report from the 1996 NCEER and 1998 NCEER/NSF workshops on evaluation of liquefaction resistance of soils. *Journal of Geotechnical and Geoenvironmental Engineering*, *ASCE* **124:10**, 817-833.
Zhou, Y.G. (2007). Soil structure: The shear wave velocity-based characterization and its effects on dynamic behavior. Ph.D. dissertation, Zhejiang University, Hangzhou, P. R. China. (in Chinese)
Zhou, Y.G. and Chen, Y.M. (2007). Laboratory investigation on assessing liquefaction resistance of sandy soils by shear wave velocity. *Journal of Geotechnical and Geoenvironmental Engineering*, *ASCE* **138:8**, 959-972.
Zhou, Y.G. and Chen, Y.M. (2005). Influence of seismic cyclic loading history on small strain shear modulus of saturated sands. *Soil Dynamics and Earthquake Engineering* **25:5**, 341-353.
Zhou, Y.G., Chen, Y.M. and Ding, H.J. (2005). Analytical solutions to piezoelectric bimorphs based on improved FSDT beam model. *Smart Structures and Systems* **1:3**, 309-324.